J Stomatol Oral Maxillofac Surg 123 (2022) 203–208

Available online at
ScienceDirect
www.sciencedirect.com

Elsevier Masson France
EM|consulte
www.em-consulte.com

Original Article

Evaluation of different fixation methods with finite element analysis in total mandibular subapical osteotomy

Elçin BEDELOĞLU, [a], Mustafa YALÇIN, [b]*

[a] Istanbul Aydın University, Faculty of Dentistry, Department of Oral and Maxillofacial Surgery, Istanbul, Turkey
[b] Associate Professor, Istanbul Kent University, Faculty of Dentistry, Department of Oral and Maxillofacial Surgery, Istanbul, Turkey

A R T I C L E I N F O

Article History:
Received 25 April 2021
Accepted 11 May 2021
Available online 16 May 2021

Keywords:
Mandible
Subapical osteotomy
Miniplate
Stress distribution

A B S T R A C T

Purpose: The purpose of the study was to evaluate the stress distribution in various miniplates that were used in cases that underwent advancement with total mandibular subapical osteotomy (TMSO) using finite element analysis (FEA).
Material and method: Cone beam computed tomography (CBCT) images of a patient with appropriate bone tissues were used as a reference for the modeling of the mandible. In all mandibular models, horizontal TMSO was performed in a region 5 mm away from the apex of the teeth and vertical TMSO was performed in the retromolar region, 10 mm posterior to the second molar tooth. After TMSO, the dentoalveolar segment was advanced 3 mm and miniplates were placed symmetrically at four points for fixation. Four different miniplates with 2.0 mm thickness were used. Three different forces were applied to the models. Stress distribution on the models was evaluated using maximum von Mises stress values.
Results: The maximum von Mises stress occurred in *Y + I* and *Y + L* models following the application of 300 N force from the incisal. An evaluation of posterior unilateral force indicated that the stress was remarkably high in the models with a posterior I-plate. The stress in the *Y + I* model was higher under unilateral force compared to the stress in other models. Under posterior bilateral force, the maximum von Mises stress values occurred in the I-plates of *T + I, Y + I*, and *L + I* models (1006, 1012, and 1004 MPa, respectively).
Conclusion: Within the limitations of our study, we found that the ideal stress distribution was in the *T + L* and *L + L* plate combinations in the plates used for fixation after advancement with TMSO.

1. Introduction

Lefort 1 and sagittal split osteotomy (SSO) are commonly used in the treatment of dentofacial deformities [1]. SSO is often administered in cases requiring advancement, retrusion, and rotation [1,2]. In addition to SSO, other techniques such as segmental osteotomies (anterior segmental subapical osteotomy) and total subapical osteotomies can also be indicated in patients [3,4]. Surgical interventions such as mandibular advancement and set-back surgery, augmentation, and rotation of the dentoalveolar segment of the mandible can be performed using segmental or total subapical osteotomies.

Total mandibular subapical osteotomy (TMSO) first was defined by McIntosch in 1974, for management of anterior open bite and dentoalveolar retrusion or protrusion with inconsistency between the chin and the lower lip [5,6]. TMSO was performed in various cases such as anterior open bite, sagittal split osteotomy relapse, lateral open bite, class II division I cases with normal chin position, mandibular height deficiency with normal pogonion point, and class II division II cases requiring a change in mentolabial sulcus [4,5,7-11].

Although TMSO was described long years ago, there are a limited number of studies and case reports in the literature investigating the effectiveness of TMSO. Even though there have been several biomechanical studies evaluating different fixation methods used in mandibular anterior segmental osteotomy [12,13], to our knowledge, there is no biomechanical study investigating different fixation methods used in TMSO. In this study, we evaluated the stress distribution in various miniplates that were used in cases that underwent advancement with TMSO using finite element analysis (FEA).

2. Materials and methods

This research was conducted through collaboration between Istanbul Aydın University Faculty of Dentistry and Ay Tasarim Ltd.

A computer equipped with Intel Xeon ® R CPU 3.30 GHz processor, 500 GB Hard disk, 14 GB RAM, and Windows 7 Ultimate Version Service Pack 1 operating system, an Activity 880 (Smart optics Sensortechnik GmbH, Sinterstrasse 8, D-44,795 Bochum, Germany) optical 3D scanner, Rhinoceros 4.0 3D modeling software (3670 Woodland

* Corresponding author.
E-mail address: myalcin.omfs@gmail.com (M. YALÇIN).

https://doi.org/10.1016/j.jormas.2021.05.006
2468-7855/

Park Ave N, Seattle, WA 98,103 USA), VRMesh Studio (VirtualGrid Inc, Bellevue City, WA, USA) and Algor Fempro (ALGOR, Inc. 150 Beta Drive Pittsburgh, PA 15,238–2932 USA) analysis software was used to design and homogenize a 3D network structure and to create a 3D solid model to perform FEA. Models were created geometrically with VRMesh Studio and then transferred to Algor Fempro software in the STL file format for analysis.

2.1. Modeling

Cone beam computed tomography (CBCT) images of a patient with appropriate bone tissues were used as a reference for the modeling of the mandible. All the images were obtained using a 3 M Iluma CBCT scanner. The images were transferred to the 3D-doctor software, on which bone tissues were separated based on their Hounsfield unit (HU) values using the "Interactive Segmentation" method. Following the separation process, a 3D model was obtained using the "3D Complex Render" method. Spongious bone was obtained from the bone tissue using the offset method and force transfer was achieved by performing necessary adjustments. The modeling procedure was completed by placing all models into the three-dimensional space with correct coordinates in the Rhinoceros software.

The stresses on the models were reported according to the von Mises stress values, which are the initial values of deformation energy indicating the stress distribution in FEA [14]. Material values (elastic modulus and Poisson's ratio), which define the physical properties of the structures in the models, were entered to the software program (Table 1). In the software program, solid body properties were accepted as linear elastic, homogeneous, and isotropic. Since the values obtained as a result of FEA were the results of mathematical calculations without variance, no statistical analyses could be made.

2.2. Osteotomy and miniplate fixation

In all mandibular models, horizontal TMSO was performed in a region 5 mm away from the apex of the teeth and vertical TMSO was performed in the retromolar region, 10 mm posterior to the second molar tooth. After TMSO, the dentoalveolar segment was advanced 3 mm and miniplates were placed symmetrically at four points for fixation.

The insertion points of miniplates were determined as bilateral canine and first molar area. Four different miniplates with 2.0 mm thickness were used in the study:

1. T-plate
2. Y-plate
3. L-plate
4. I-plate, (Fig. 1)

Following the insertion of the plates, six study models were created, among which T-, Y- and L- plates were used in the anterior and L- and I-plates were used in the posterior region, as shown below:

1. Bilateral anterior T-plate, posterior I-plate (*T+I* model)
2. Bilateral anterior T-plate, posterior L-plate (*T+L* model)

Table 1
Material properties.

	Elasticity modulus (Mpa)	Poisson's ratio
Dentin	15,000	0.31
Enamel	80,000	0.3
Cortical bone	13,800	0.26
Spongious bone	1345	0.3
Miniplates and screws	110,000	0.35

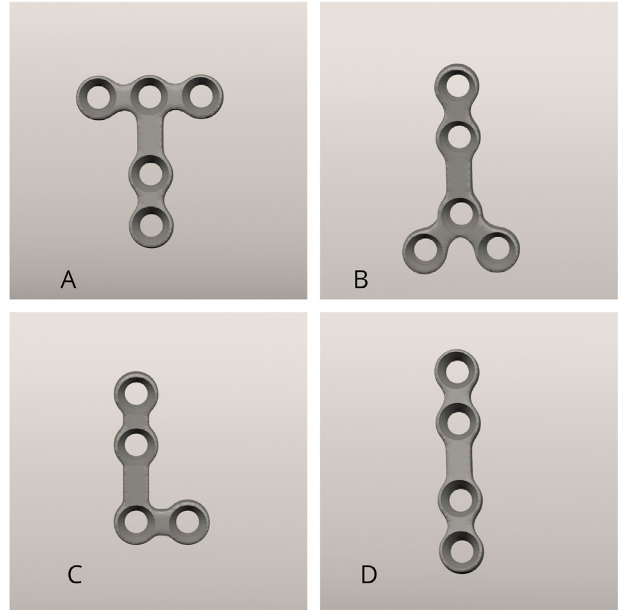

Fig. 1. Miniplates. A) T-plate, B) Y-plate, C) L-plate, D) I-plate.

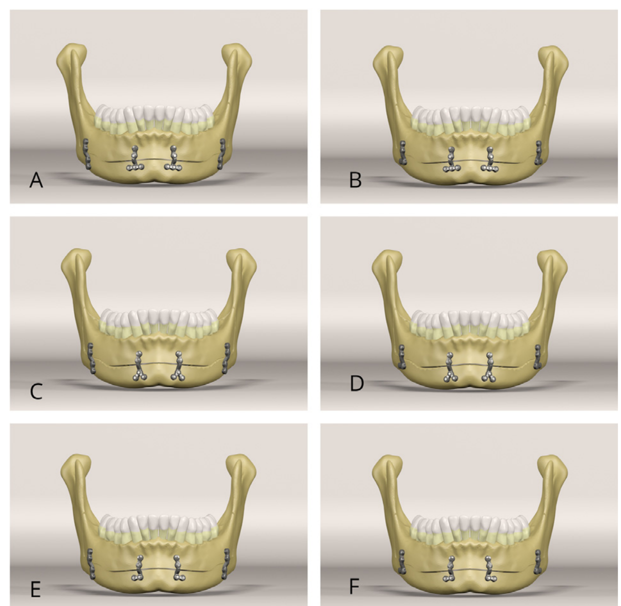

Fig. 2. Experimental mandible models. A) *T+I* model, B) *T+L* model, C) *Y+I* model, D) *Y+L* model, E) *L+I* model, F) *L+L* model.

3. Bilateral anterior Y-plate, posterior I-plate (*Y+I* model)
4. Bilateral anterior Y-plate, posterior L-plate (*Y+L* model)
5. Bilateral anterior L-plate, posterior I-plate (*L+I* model)
6. Bilateral anterior L-plate, posterior L-plate (*L+L* model), (Fig. 2)
7. All the plates were adapted to the models advanced by TMSO (the plates were bent and then adapted to the model) and then fixed using 7 mm screws (Fig. 3). All the models were fixed from the lower margin of the mandible and the condylar region to have 0 degree of freedom (DOF) motion (Fig. 4).

2.3. Force application

Three different forces were applied to the models:

1. 300 N vertical force from the incisal of the mandibular anterior teeth (150 N on the right first incisor and 150 N on the left first incisor)

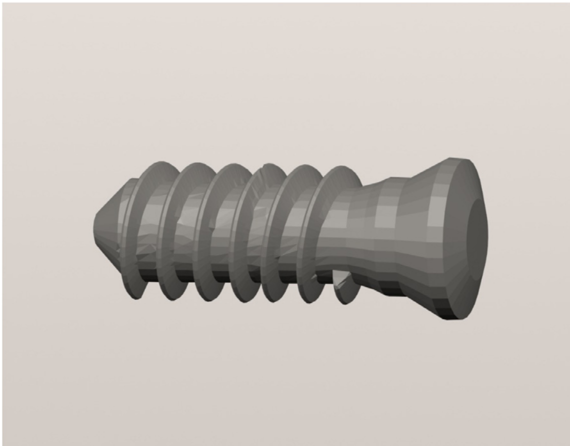

Fig. 3. Miniplate screw with 7 mm length.

2. 300 N vertical force from the occlusal of the unilateral first molar
3. 300 N force from the occlusal of each bilateral first molar (600 N force in total), (Fig. 4)

In each model, the stresses occurring on the miniplates after the application of occlusal forces were evaluated using maximum von Mises stress values (Fig. 5).

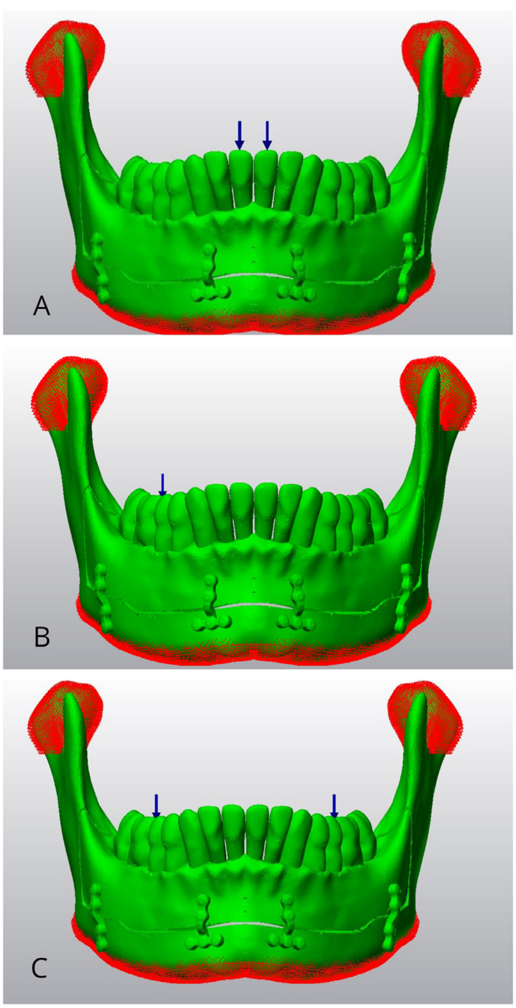

Fig. 4. Boundary conditions and occlusal forces. A) Incisal force, B) Unilateral posterior occlusal force, C) Bilateral posterior occlusal force.

3. Results

The results indicated that the maximum von Mises stress occurred in *Y+I* and *Y+L* models following the application of 300 N force from the incisal, and the stress values for both models were 605 MPa in the right Y-plate and 639 MPa in the left Y-plate. The lowest stress value in anterior plates occurred in the *T+I* and *T+L* models with a T-plate, and their approximate value was 254 MPa. The lowest stress in posterior plates was in the *Y+L* model (96.50 MPa), (Fig. 6).

An evaluation of posterior unilateral force indicated that the stress was remarkably high in the models with a posterior I-plate (*T+I*, *Y+I*, *L+I* models) and was the lowest in the models with a posterior L-plate. While the stress in anterior Y-plates (*Y+I*, *Y+L* models) was the highest, the stress in the T- and L-plates was lower. The stress in the *Y+I* model was higher under unilateral force compared to the stress in other models (Fig. 7).

Under posterior bilateral force, the maximum von Mises stress values occurred in the I-plates of *T+I*, *Y+I*, and *L+I* models (1006, 1012, and 1004 MPa, respectively). The maximum stress values in anterior plates occurred in *Y+I* (550 MPa) and *Y+L* (587 MPa) models. The stress values in anterior T- and L-plates are shown in Fig. 8. Among all models, *T+L* and *L+L* had the lowest and most balanced stress distribution (Fig. 8).

4. Discussion

Finite element stress analysis (FEA) is a numeric method frequently used for biomechanical evaluations in dentistry and maxillofacial surgery and in determining the magnitude and distribution of stress on miniplates, screws, and reconstruction plates used in osteosynthesis. To date, numerous fixation methods and materials used after fracture, orthognathic surgery, and other osteotomies have been developed [12,13,15-17]. In some studies, FEA has been used for the evaluation of fixation methods and the stresses occurring after orthognathic surgery and fractures of the mandible (mandibular angulus, symphysis, condylar fractures) [16,17]. Among the FEA studies that evaluated fixation methods after segmental or total subapical osteotomy, the study by Kilinc et al. simulated a 3- and 5-mm superior repositioning of mandibular anterior segmental osteotomy and created three different finite element models corresponding to different fixation techniques for each superior repositioning [12,13]. In the limited number of clinical studies on TMSO, researchers used different fixation methods and miniplates but did not evaluate the fixation methods biomechanically [1,2,4]. On the other hand, some other studies employed various modifications and approaches in the application of miniplates in TMSO. Among these, Konopnicki et al. [1] used bilateral T-plates anteriorly and applied the I-plate in the posterior molar region. Another researcher applied horizontal I-plates posteriorly [4]. Cavalcante et al. [2], on the other hand, applied bilateral L-plates in the anterior region only.

In clinical studies administering TMSO, repositioning procedures such as advancement, rotation, and augmentation can be applied to the dentoalveolar segment after different indications, which, as a result, may require different fixation methods and materials [1,2,8,10]. In our study, 3-mm advancement was applied with TMSO and no augmentation or rotation was performed. In each model, four miniplates were applied, including two miniplates in the anterior and two miniplates in the posterior region. To facilitate the adaptation of the miniplates to the models after advancement, the miniplates were inserted in the models and fixed after bending. We consider that the fixation methods used in different indications cannot be evaluated clinically and biomechanically in accordance with standardization since there have been clinical studies in the literature that applied TMSO with different indications [1,2,8,10,18]. For

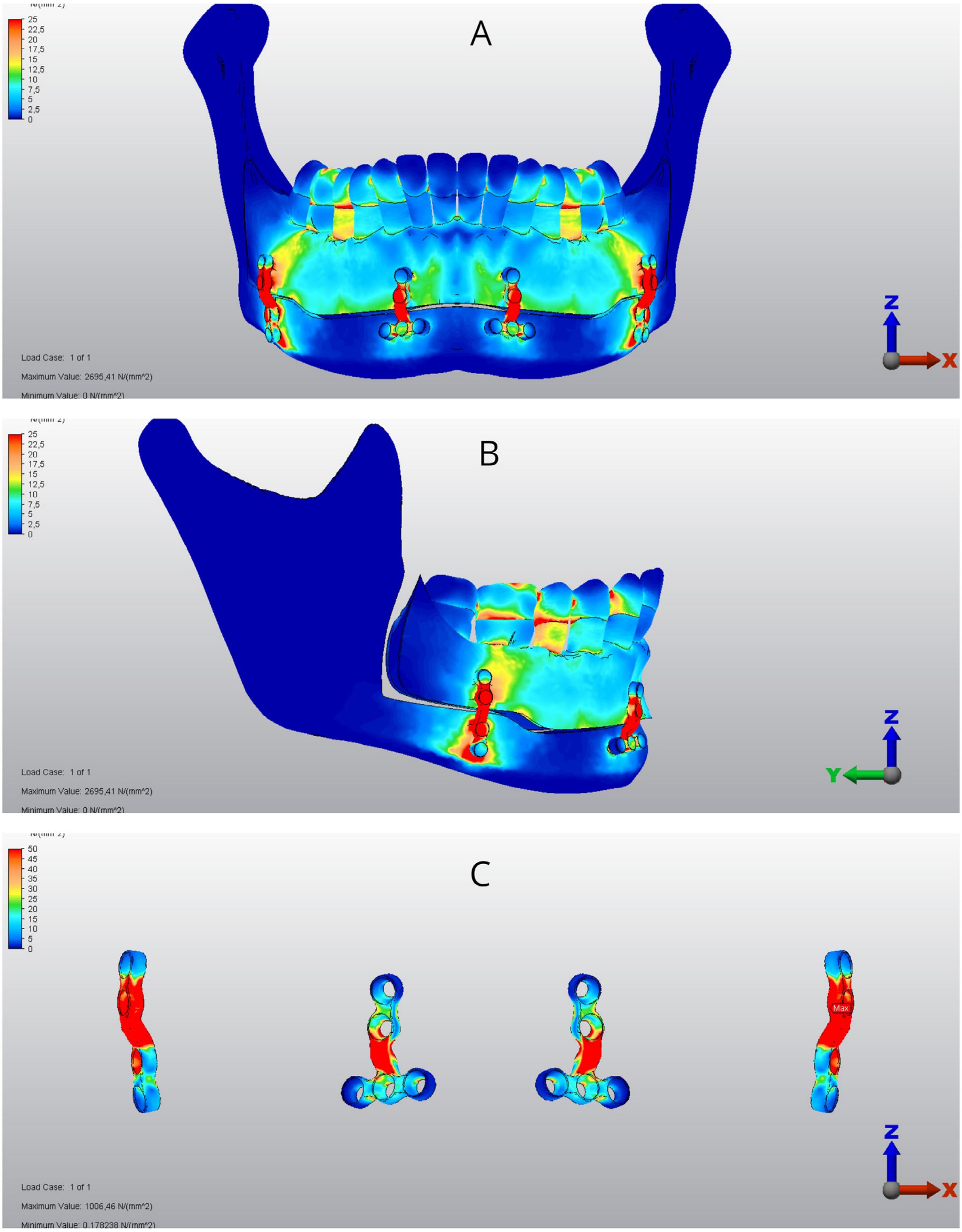

Fig. 5. Anterior (A) and lateral (B) aspect of the experimental model. (C) Stress distribution on the miniplates after the application of occlusal forces.

this reason, our study only included TMSO cases that underwent advancement alone. Future studies evaluating biomechanical features of fixation methods applied for other TMSO cases may guide clinicians.

In our study, the L- or I-plate was preferred for the posterior region in all models. Under anterior force, the stress in the I-plate was approximately 30% higher than in the L-plate in all models. In the stress distribution of T-, Y-, L-plates used in the anterior region, the stress in the Y-plate was approximately twice higher than that of L- and T-plates. The most balanced and minimum stress distribution under anterior forces in all models was seen in the *T* + *L* model (Fig. 6).

Under unilateral force, the stress in the *Y* + *I* model was higher than in all other models. In posterior I-plates, the stress was approximately 20% higher on the side where force was applied and was 40% high in the non-force side compared to the L-plates. The stress in

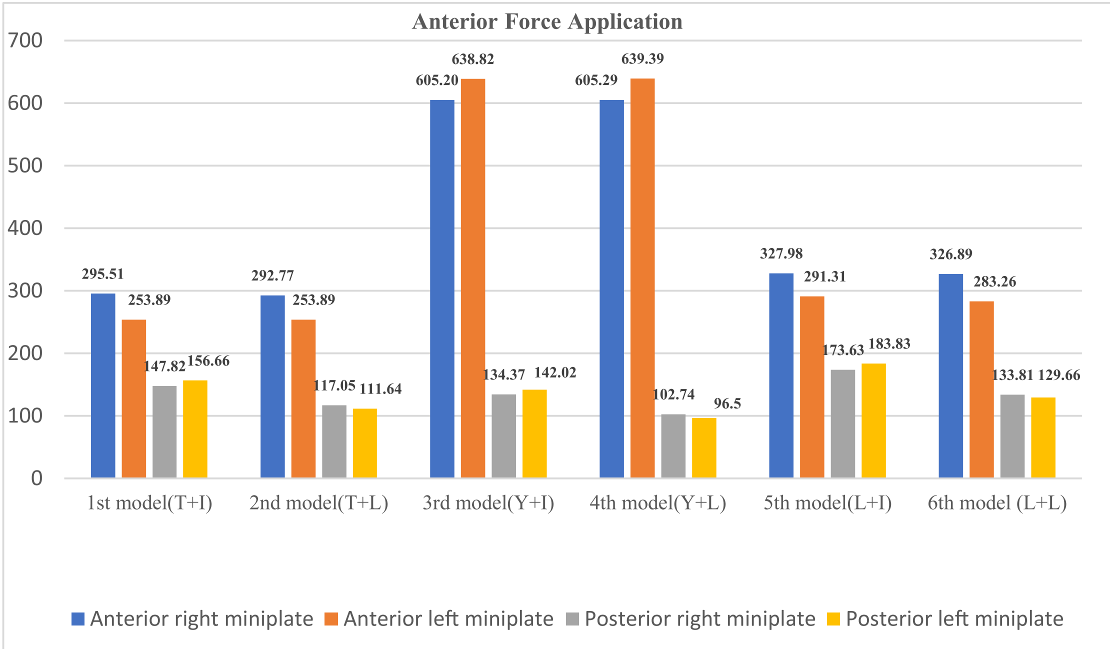

Fig. 6. Distribution of von Mises stress after anterior incial force on experimental models (MPa).

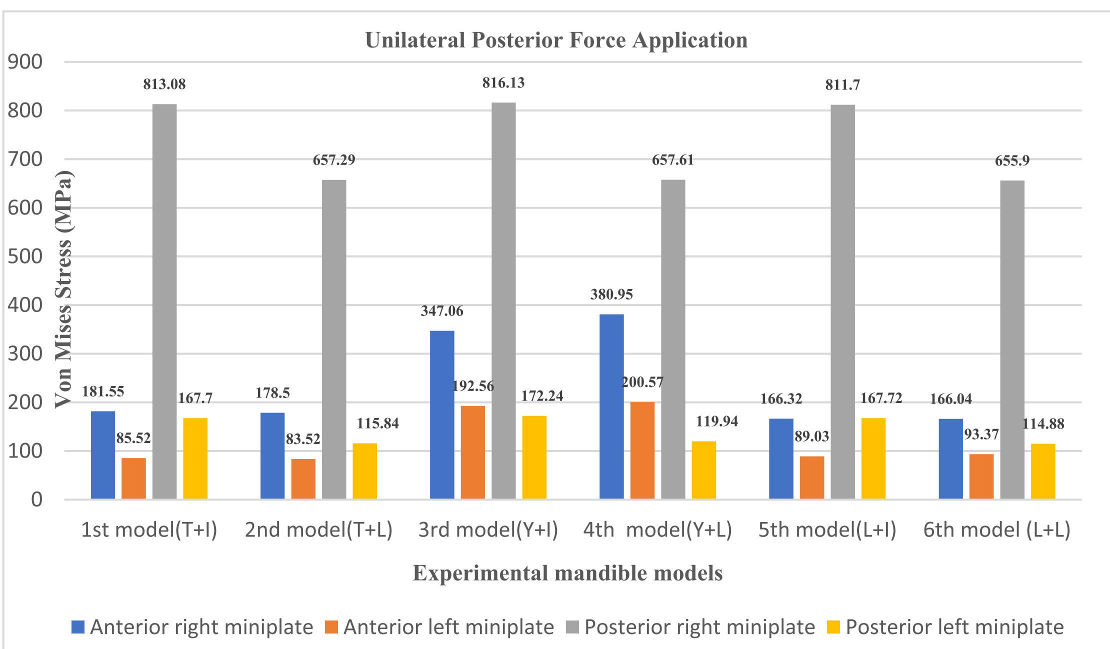

Fig. 7. Distribution of von Mises stress after unilateral posterior occlusal force on experimental models (MPa).

anterior Y-plates, as in anterior bite force, was twice higher than that of T- and L-plates. The lowest and balanced stress distribution was seen in *T+L* and *L+L* models and the stress distribution in these two models was similar (Fig. 7).

Under bilateral force, the stress in the I-plates was approximately 30% higher than in the L-plates in all models. In the anterior region, the stress in Y-plates was about 70% higher than in T- and L-plates (Fig. 8).

Increased stress in miniplates can lead to stress accumulation in screws and bone resorption, miniplate fractures, and osteosynthesis failure. Therefore, using plate systems that will ensure a balanced and minimal stress on the miniplates is clinically important.

5. Conclusion

Within the limitations of our study, we found that the ideal stress distribution was in the *T + L* and *L + L* plate combinations in the plates used for fixation after advancement with TMSO. In addition, the

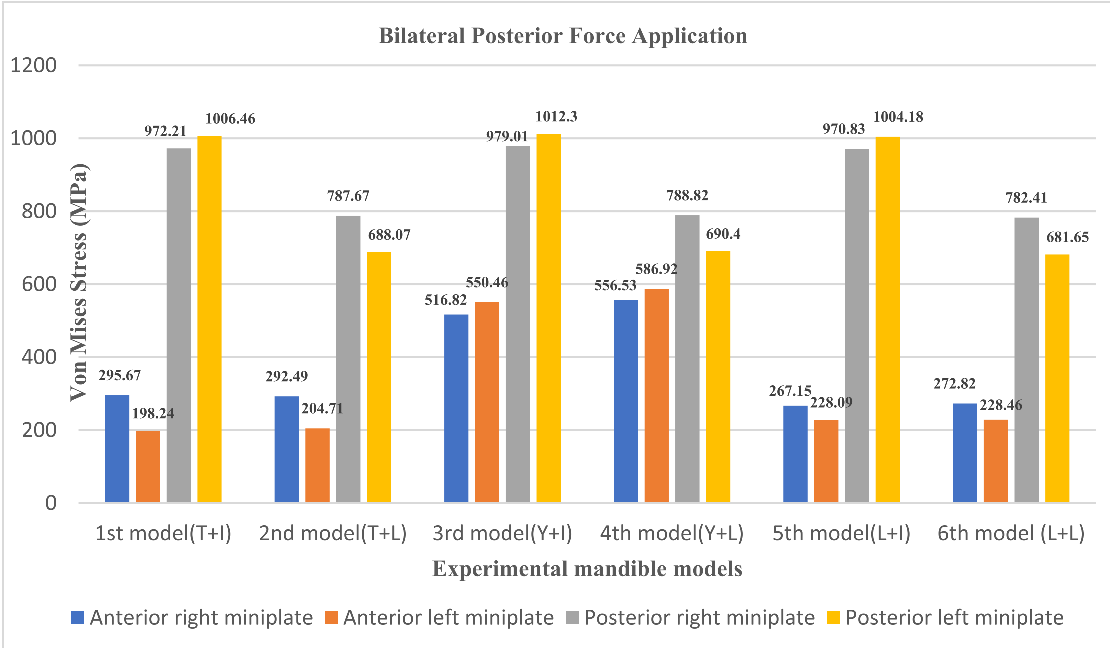

Fig. 8. Distribution of von Mises stress after bilateral posterior occlusal force on experimental models (MPa).

stress values in the Y-plate in the anterior region and in the I-plate in the posterior region were the highest under all forces.

Author's contribution

Elçin Bedeloğlu: Data collection, management and analysis
Mustafa Yalçın: Manuscript writing and editing

Ethical approval

There was no need ethical approval due to the nature of the study.

Declaration of Competing Interest

The authors declare that they have no conflict of interest.

Funding

None.

References

[1] Konopnicki S, Nicot R, Schlund M, Ferri J. Total Mandibular subapical osteotomy to correct Class II with inferior alveolar retrusion. Int Orthod 2019;17(1):114–22. doi: 10.1016/j.ortho.2019.01.011.
[2] Cavalcante RC, Bergamaschi IP, Sebastiani AM. Total mandibular subapical alveolar osteotomy to correct class II division I dentofacial deformity. Case Rep Surg 2018;2018:5469481. doi: 10.1155/2018/5469481.
[3] Sahin T, Garreau E, Komakli Y, Nicot R, Sciote JJ, Ferri J. Mandibular anterior segmental subapical osteotomy for incisor axis correction. J Stomatol Oral Maxillofac Surg 2017;118(5):271–8. doi: 10.1016/j.jormas.2017.06.005.
[4] Boye T, Doyle P, McKeown F, Sandler J. Total subapical mandibular osteotomy to correct class 2 division 1 dento-facial deformity. J Craniomaxillofac Surg 2012;40(3):238–42. doi: 10.1016/j.jcms.2011.04.010.
[5] MacIntosh RB. Encouraging experiences with an infrequently indicated procedure. J Maxillofac Surg 1974;2(4):210–8.
[6] Buckley MJ, Turvey TA. Total mandibular subapical osteotomy: a report on long-term stability and surgical technique. Int J Adult Orthodon Orthognath Surg 1987;2(3):121–30.
[7] Bell WH, Jacobs JD, Legan HL. Treatment of class II deep bite by orthodontic and surgical means. Am J Orthod 1984;85(1):1–20. doi: 10.1016/0002-9416(84)90118-0.
[8] Booth DF, Dietz V, Gianelly AA. Correction of class II malocclusion by combined sagittal ramus and subapical body osteotomy. J Oral Surg 1976;34(7):630–4.
[9] Herford A.S., Stringer D.E., Tandon R., "Orthognathic surgery," an issue of oral and maxillofacial clinics of North America, pp. 480–492, Elsevier, 2004.
[10] Mohammed-Ali RI, Schache A, Walsh S, Sneddon K. Total mandibular subapical osteotomy: modification of the technique. Br J Oral Maxillofac Surg 2009;47(8):629–30. doi: 10.1016/j.bjoms.2008.11.017.
[11] Pangrazio-Kulbersh V, Berger JL, Kaczynski R, Shunock M. Stability of skeletal Class II correction with 2 surgical techniques: the sagittal split ramus osteotomy and the total mandibular subapical alveolar osteotomy. Am J Orthod Dentofacial Orthop 2001;120(2):134–43.
[12] Kilinç Y, Erkmen E, Kurt A. Biomechanical evaluation of different fixation methods for mandibular anterior segmental osteotomy using finite element analysis, part one: superior repositioning surgery. J Craniofac Surg 2016;27(1):32–5. doi: 10.1097/SCS.0000000000002172.
[13] Kilinç Y, Erkmen E, Kurt A. Biomechanical evaluation of different fixation methods for mandibular anterior segmental osteotomy using finite element analysis, part two: superior repositioning surgery with bone allograft. J Craniofac Surg 2016;27(1):36–40. doi: 10.1097/SCS.0000000000002173.
[14] Singley JE, Mishke CR. Mechanical Engineering Design. 5th ed. New York: McGraw-Hill Book Company; 1989.
[15] Sommerfeld R, Bergamaschi IP, Scariot R, da Costa DJ. Evaluation of tissue tensions in segmental maxillary osteotomies by finite element analysis. J Oral Maxillofac Surg 2020;78(12):2298.e1–2298.e9. doi: 10.1016/j.joms.2020.07.002.
[16] Ergezen Ozasir E, Tosun E, Tuz HH. Evaluation of the effect of mandibular length and height on the sagittal split ramus osteotomy rigid internal fixation techniques: A finite element analysis. J Stomatol Oral Maxillofac Surg 2020;121(6):652–7. doi: 10.1016/j.jormas.2020.02.003.
[17] Liokatis P, Tzortzinis G, Gerasimidis S, Smolka W. Finite element analysis of different titanium plates for internal fixation of fractures of the mandibular condylar neck. J Oral Maxillofac Surg 2021;79(3):665.e1–665.e10. doi: 10.1016/j.joms.2020.09.038.
[18] Scolozzi P, Herzog G. Total mandibular subapical osteotomy and Le Fort I osteotomy using piezosurgery and computer-aided designed and manufactured surgical splints: a favorable combination of three techniques in the management of severe mouth asymmetry in Parry-Romberg syndrome. J Oral Maxillofac Surg 2014;72(5):991–9.